COMMUNICATION

Enhancing electrocatalytic hydrogen evolution by nickel salicylaldimine complexes with alkali metal cations in aqueous media†

Haiyan Shao,[abc] Subas K. Muduli,[ad] Phong D. Tran‡[c] and Han Sen Soo*[abc]

New salicylaldimine nickel complexes, comprising only earth-abundant elements, have been developed for electrocatalytic hydrogen evolution in aqueous media. The second-sphere ether functionalities on the periphery of the complexes enhance the electrocatalytic activity in the presence of alkali metal cations. The electrocatalysts demonstrate improved performances especially in the economical and sustainable seawater reaction medium.

Global climate change has been widely attributed to the rampant consumption of fossil fuels and has stimulated recent efforts to develop alternative, more sustainable sources of fuels. An attractive solution is to develop artificial photosynthetic systems that can harvest sunlight, like a leaf, and store the solar energy in the form of chemical bonds in hydrogen (H_2) and oxygen (O_2) *via* water splitting. Energy storage is appealing since sunlight is intermittent. When alternative energy resources such as sunlight or geothermal energy can be efficiently converted into electricity, a critical challenge in creating a practical artificial photosynthetic system will be to develop commensurately efficient electrocatalysts for H_2 evolution from seawater.[1–4]

Platinum (Pt) is a well-known electrocatalyst for the reduction of protons (H^+) to H_2 in commercial electrolysers, with a low overpotential (η), long durability, and high turnover frequency (TOF).[3] However, Pt is a precious metal, partly due to its relative

scarcity in the Earth's crust. Consequently, more earth-abundant, heterogeneous electrocatalysts have been sought and reported, including metal chalcogenides,[5–7] carbides,[8] phosphides,[9–11] and hydroxides,[12,13] in attempts to produce H_2 at prices competitive with those in the production from fossil fuels.

Concurrent with the research on heterogeneous catalysts, a number of molecular complexes consisting of earth-abundant elements have been found to be exceptional H_2 evolution electrocatalysts. These complexes display especially impressive TOFs in organic solvents, some of which surpass the activities of natural hydrogenase enzymes, and are supported by ligands including N_2P_2,[14–17] macrocyclic oximes,[18–20] polypyridines,[21,22] thiolates,[23–26] and porphyrins.[27] A select few of the molecular electrocatalysts are active in aqueous media and ligated by scaffolds including $PY5Me_2$,[28] DPA-Bpy,[29] and P_4N_2.[30] Co salicylaldimine catalysts have also been used for photodriven H_2 evolution in water.[31] Among the most active catalysts, a common feature has been the judicious customisation of the second coordination sphere *via* the introduction of bioinspired H^+ relays. These complexes poise the Lewis basic amine and Bronsted acidic alcohol groups in close proximity to the redox-active metal centre, similar to natural enzymatic systems. However, few studies have documented the effects of alkali metal ions in the second coordination sphere of molecular H_2 evolution electrocatalysts, although copious amounts of alkali metal cations are found in seawater and biological systems.

Herein, we describe the H_2 evolution activity of new nickel (Ni) complexes supported by salicylaldimine ligands with pendant, chelating ether groups that can bind Lewis acids such as alkali metal cations. The alkali metal ion-binding capabilities of salen-type ligands without pendant ether functionalities have been previously observed in molecular CO_2 complexes.[32] The role of alkali metal cations is important since they constitute the most practical and cheapest electrolytes, and will be especially relevant if seawater (Na^+) is to become the ultimate aqueous medium for large-scale H^+ reduction.

We demonstrate that our water-soluble Ni electrocatalysts, which are readily accessible in a few steps from commercially

a Division of Chemistry and Biological Chemistry, School of Physical and Mathematical Sciences, Nanyang Technological University, Singapore 637371, Singapore. E-mail: hansen@ntu.edu.sg
b Singapore-Berkeley Research Initiative for Sustainable Energy (SinBeRISE), 1 Create Way, Singapore 138602, Singapore
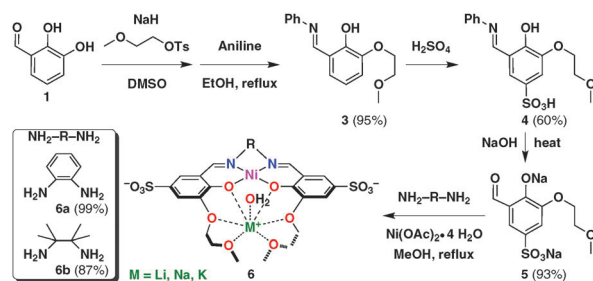*c Solar Fuels Laboratory, Nanyang Technological University, 50 Nanyang Avenue, Singapore 639798, Singapore*
d Energy Research Institute@NTU (ERI@N), Nanyang Technological University, Research Techno Plaza, Singapore 637553, Singapore

‡ Current address: Department of Advanced Materials Science and Nanotechnology, University of Science and Technology of Hanoi (Vietnam France University), 18 Hoang Quoc Viet, Cau Giay, Hanoi, Vietnam.

Scheme 1 Synthesis of Ni catalysts (**6**) with pendant ether groups.

Fig. 1 CVs of (a) 1.0 mM of **6a** in 0.10 M n-Bu_4NPF_6 in DMF with different concentrations of TFA; (b) 1.0 mM **6a** in 0.10 M Na_2SO_4 with different HOAc concentrations at scan rates of 100 mV s^{-1} with a glassy carbon working electrode (3 mm diameter).

available chemicals (Scheme 1), behave as H_2 evolution catalysts in both neutral and acidic aqueous solutions. Moreover, the chelating methoxyethoxy group can bind hydrated alkali metal cations to provide hydrogen-bonding stabilisation and enhanced electrocatalytic proton reduction reactivity.

The ligands were prepared by adaptations of previously reported methods.[33–35] Compound **3** and subsequent organic molecules and Ni complexes are new and their syntheses and characterisation are included in the ESI.† The Ni complexes (**6**) were prepared by condensation of aldehyde **5**, a diamine, and nickel acetate with high yields (Scheme 1). Two design elements were introduced to enhance H_2 evolution from saline aqueous media: (i) introduction of sulfonate groups to improve water solubility and (ii) attachment of pendant, non-coordinating ether functionalities as hard Lewis bases for alkali metal cations. The salicylaldimine framework is highly modular and synthetically accessible; the amine and the aldehyde can be independently optimised and derivatised. Two distinct complexes **6** (diamine = o-phenylenediamine, **6a**; diamine = 2,3-dimethylbutane-2,3-diamine, **6b**) were prepared to compare their activities.

Both complexes have been characterised by NMR spectroscopy, high-resolution mass spectrometry, and elemental analyses. The deep orange **6a** displays bands at 216, 312, 360, and 486 nm ($\varepsilon = 2.48 \times 10^4$, 1.03×10^4, 1.19×10^4 and 3.13×10^3 M^{-1} cm^{-1}, respectively, Fig. S1, ESI†), which have been used to gauge the stability of **6a** under catalytic conditions (*vide infra*). Complex **6b** functions similarly to **6a**, with lower electrocatalytic activity. All subsequent studies have thus been performed with **6a**. Although we have not been able to grow single crystals of **6a** or **6b**, we were able to prepare **6c**, which has the same structure as **6a** without the sulfonate groups. Unlike numerous dimeric or polymeric Ni salen complexes,[33] **6c** is mononuclear (Fig. S2, ESI†).[36] The salient structural parameters are listed in Tables S1–S10 (ESI†). The coordination geometry around Ni is square planar, in accordance with the d^8 electronic configuration. Notably, the pendant ether arms cradle one K^+ cation similar to previous reports with Na^+ (other examples in the ESI†),[36] potentially directing the solvent molecules in close proximity to the Ni centre. Although this only represents the solid-state structure, the UV-vis (Fig. S3, ESI†) and electrochemical experiments suggest that the alkali metal cations indeed influence the second coordination sphere around Ni in water during H_2 evolution catalysis (Scheme S1, ESI†).

The cyclic voltammogram (CV, Fig. S4, ESI†) of **6a** in N,N-dimethylformamide (DMF) features a quasi-reversible redox couple
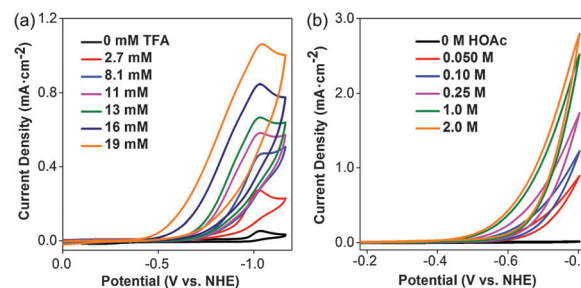
at −1.04 V *vs.* NHE assigned to a metal-based Ni^{II}/Ni^{I} redox couple. The redox wave becomes increasingly reversible at scan rates up to 1.0 V s^{-1}, which may be due to the structural reorganisation or precipitation of the triply anionic transient species on the electrode.[37,38] In the presence of acetic acid (HOAc) as a weak proton donor in DMF, the CVs show moderate current increases with little change to the onset current (Fig. S5, ESI†), indicating that **6a** behaves as an electrocatalyst for H_2 evolution even with weak acids. When the stronger trifluoroacetic acid (TFA) was used as the proton source, the CV displayed a dramatic increase in the catalytic current over the background (Fig. 1a), with an anodic shift of the onset current. After varying the concentration of TFA added, the CVs reveal a 2nd order dependence on the acid concentration (Fig. S6, ESI†).[14] Attempts to perform a foot-of-the-wave analysis[39] on H_2 evolution in the presence of TFA have been complicated by significant deviations from linearity due to the anodic onset shift at higher TFA concentrations (Fig. S7, ESI†). This onset shift could be due to equilibrium protonation of the phenoxide donor at high acid concentrations (ESI†),[40] which reduces the overpotential required for electrocatalytic H_2 evolution by positioning protons in close proximity to the Ni centre. Instead, the foot-of-the-wave analysis using acetic acid as the proton donor demonstrates the expected linear behaviour, yielding an apparent rate constant of 17.9 M^{-1} s^{-1} in 0.10 M acetic acid at a scan rate of 100 mV s^{-1} (Fig. S8, ESI†).

Interestingly, the CV of **6a** in neutral water with Na_2SO_4 as the electrolyte exhibits a remarkable increase in the catalytic current at an onset of −1.05 V *vs.* NHE, corresponding to an overpotential of 0.59 V.§ Gas bubbles are also observed during cathodic scans. The overpotential of **6a** is comparable to or lower than that of the other molecular electrocatalysts that contain first-row transition metals and function in neutral water with glassy carbon working electrodes.[41] For instance, the overpotentials for Co complexes ligated by P_4N_2 ligands[30] or DPA-Bpy[29] are about 0.55 and 0.78 V, respectively, with glassy carbon working electrodes. When 0.10 M aqueous acetic acid is used (pH = 2.8), the catalytic onset shifts to −0.64 V, which is larger than the expected Nernstian shift of about 0.24 V due to an increase in [H^+] by about four orders of magnitude (Fig. 1b). In addition, the catalytic current shows a 1st order dependence on the concentration of **6a** (Fig. 2a), suggesting that H_2 evolution occurs *via* the protonation of a mononuclear Ni intermediate,
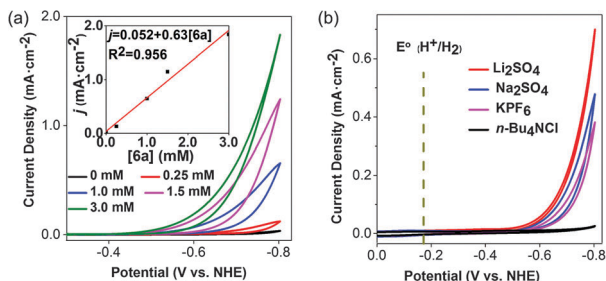
Fig. 2 CVs of (a) different concentrations of **6a** complex in 0.10 M Na_2SO_4, 0.10 M HOAc solution. Inset: Linear relationship between current density j and [**6a**] at −0.80 V; (b) 1.0 mM **6a** in 0.10 M of different electrolytes in 0.10 M HOAc at scan rates of 100 mV s^{-1} with a glassy carbon electrode (3 mm diameter).

rather than bimolecular coupling of two highly anionic Ni complexes (Scheme S1, ESI†).[42]

To explore the effects of the pendant ether on **6a**, CVs have been conducted in the presence of n-Bu$_4$NCl, Li$_2$SO$_4$, Na$_2$SO$_4$, and KPF$_6$ as the electrolytes in 0.10 M acetic acid (Fig. 2b). With n-Bu$_4$N$^+$ as the electrolyte, the current density increases 0.70 mA cm^{-2} above the background current at an overpotential of 0.84 V in the electrolyte solution with no added acids (Fig. S9d, ESI†). This indicates an appreciable, but slow H$_2$ evolution reaction. The n-Bu$_4$N$^+$ cation is bulky and may hinder the access to the Ni catalytic centre by hydronium ions, similar to the proton-gated hangman iron porphyrins reported by Nocera *et al.*[43] In contrast, with Na$_2$SO$_4$ as the electrolyte, the current density is 8.2 times the catalytic current with n-Bu$_4$N$^+$ as the electrolyte (Fig. S9, ESI†). We observe the highest electrocatalytic current with Li$^+$ as the electrolyte (11 times compared to n-Bu$_4$N$^+$ as the electrolyte, Fig. S9, ESI†) among the common and affordable cations examined. This dramatic increase in catalytic current highlights the non-innocence of the electrolyte in our H$_2$ evolution system, and emphasises the need for prudent management of second sphere effects around the catalytic centre (Scheme S1, ESI†).[44–46] In 0.10 M acetic acid, the electrocatalytic current increase also followed the same trend (Fig. S10, ESI†). The most Lewis acidic Li$^+$ corresponds to the fastest catalytic behaviour. The Li$^+$ with the highest charge density could more effectively introduce rigidity to the ether arms and direct H$^+$ to the Ni centre, or electrostatically reduce the overpotential *via* inductive effects. Since seawater contains copious amounts of Na$^+$ ions, a judicious selection of pendant chelating groups that (size)-select for Na$^+$ may prove fruitful in improving the catalytic performance of **6a** and are being explored.

In order to probe whether a heterogeneous catalyst is the major contributor of the H$_2$ evolution electrocatalysis, a series of standard electrochemical and spectroscopic experiments have been performed. The UV-vis, high-resolution mass, and ^{1}H NMR spectra (Fig. S11–S13, ESI†) before and after controlled potential electrolysis (CPE) indicate that **6a** remains intact in solution, although there may be some adsorption. There were no nanoparticles observed upon dynamic light scattering (DLS) measurements in the electrolyte solution after CPE for 2.5 h (Fig. S14, ESI†). The UV-vis spectra in Fig. S10 (ESI†) show that

the concentration of **6a** decreased to 90% and 78% after 1 h and 2.5 h, respectively.¶ We suspected that part of **6a** was adsorbed on the carbon paper during the electrolysis process. To verify this conjecture, the used carbon paper electrodes in CPE measurements were rinsed thoroughly with water before being subjected to CPE again (Fig. S15, ESI†). The used electrode showed a small, but non-negligible amount of catalytic activity. X-ray photoelectron spectroscopy (XPS) experiments were conducted on **6a** and on the used carbon paper electrode after CPE (Fig. S16 and S17, ESI†). The data indicate that the small amounts of deposited material on the electrode have almost identical composition to **6a**, based on the XPS energies (Fig. S16 and Table S11, ESI†). We propose that some of the highly anionic **6a** is deposited on the carbon paper electrode upon reduction during catalysis, and cannot be readily rinsed off. A transmission electron microscopy (TEM) image (Fig. S18, ESI†) of the solution after CPE also exhibits little evidence of nanoparticle formation. The majority of the H$_2$ evolution electrocatalysis is still attributed to **6a** in homogeneous solution instead of deposited or suspended nanoparticles.

Controlled potential electrolysis (CPE) experiments using a mercury pool electrode have been conducted to confirm the identity of the product by gas chromatography and to gauge the stability of **6a** under catalytic conditions. The CPE measurements were performed in seawater obtained off the coast of Singapore (details in the ESI†) with a mercury pool working electrode and a carbon rod counter electrode, at an overpotential of 0.84 V. As shown in Fig. 3a, the amount of H$_2$ produced increased dramatically with a TON of 6.6 mol H$_2$ mol^{-1} catalyst cm^{-2} after 2 h, suggesting that **6a** is indeed suitable as a H$_2$ evolution catalyst with seawater as the medium. However, the Faradaic efficiency of H$_2$ production in seawater is only around 82%, since we have a one-compartment cell and some of the O$_2$ produced at the anode will be reduced at the cathode (Fig. S19, ESI†). To explore the effect of the cations in the electrolyte, CPE was also conducted with n-Bu$_4$NCl, Li$_2$SO$_4$, Na$_2$SO$_4$, KPF$_6$, and MgSO$_4$ as the electrolytes in 0.10 M acetic acid solutions (Fig. 3b). The TON with KPF$_6$ as the electrolyte was the highest in these experiments (Table S12, ESI†). We propose that the poor solubility of our Li and Mg complexes led to catalyst precipitation and amalgamation into the mercury pool electrode during CPE,
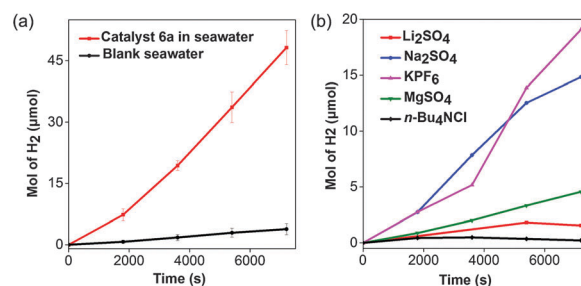

Fig. 3 The amount of H$_2$ evolved from (a) seawater with 0.22 mM catalyst **6a** (red line) and only seawater (black line); (b) 0.10 M HOAc solution with 0.25 M Li$_2$SO$_4$ (red), Na$_2$SO$_4$ (blue), and Mg$_2$SO$_4$ (green), and 0.5 M KPF$_6$ (magenta) and n-Bu$_4$NCl (black) with catalyst **6a** using a mercury pool working electrode.

which resulted in a discrepancy with the CV and CPE data that we collected using carbon-based electrodes. Nonetheless, these CPE measurements and the TON and TOF (Table S12, ESI†) confirm that **6a** remains active for electrocatalytic H^+ reduction under almost neutral, saline aqueous conditions containing Na^+ or K^+, even when mercury electrodes are used to suppress the activity of nanomaterials.

We have prepared new mononuclear Ni complexes with salicylaldimine ligands that can be used as electrocatalysts for the production of H_2 in both neutral and acidic aqueous solutions. The chelating ether groups in the structure can bind alkali metal cations to form Lewis acids and promote the H^+ reduction efficiency. Future studies will focus on the modification of the Ni complexes with electron withdrawing substituents to reduce the overpotential, applying **6a** in photocatalytic units for H_2 evolution, and grafting the molecules on semiconductors for artificial photosynthesis.[47,48]

Notes and references

§ The onset overpotential is defined as the difference between the reversible potential of the H^+/H_2 redox couple of neutral DI water (-0.46 V vs. NHE at pH 7.6) and the potential at which 10% of the current value at the peak potential was reached.

¶ The values of the charge passed during CPE were 38 and 94 C at 1 and 2.5 h, respectively, in excess of the charge needed to reduce Ni^{2+} to Ni^+ (0.12 and 0.26 C for 10% and 22% **6a** respectively).

1 Z. Han and R. Eisenberg, *Acc. Chem. Res.*, 2014, **47**, 2537–2544.
2 N. S. Lewis and D. G. Nocera, *Proc. Natl. Acad. Sci. U. S. A.*, 2006, **103**, 15729–15735.
3 D. G. Nocera, *Acc. Chem. Res.*, 2012, **45**, 767–776.
4 P. D. Tran, L. H. Wong, J. Barber and J. S. C. Loo, *Energy Environ. Sci.*, 2012, **5**, 5902–5918.
5 D. Merki, H. Vrubel, L. Rovelli, S. Fierro and X. Hu, *Chem. Sci.*, 2012, **3**, 2515–2525.
6 Y. Sun, C. Liu, D. C. Grauer, J. Yano, J. R. Long, P. Yang and C. J. Chang, *J. Am. Chem. Soc.*, 2013, **135**, 17699–17702.
7 Y. Zheng, Y. Jiao, M. Jaroniec and S. Z. Qiao, *Angew. Chem., Int. Ed.*, 2015, **54**, 52–65.
8 W.-F. Chen, C.-H. Wang, K. Sasaki, N. Marinkovic, W. Xu, J. Muckerman, Y. Zhu and R. Adzic, *Energy Environ. Sci.*, 2013, **6**, 943–951.
9 J. Kibsgaard and T. F. Jaramillo, *Angew. Chem., Int. Ed.*, 2014, **53**, 14433–14437.
10 E. J. Popczun, C. G. Read, C. W. Roske, N. S. Lewis and R. E. Schaak, *Angew. Chem., Int. Ed.*, 2014, **126**, 5531–5534.
11 M. Ledendecker, S. Krick Calderón, C. Papp, H. P. Steinrück, M. Antonietti and M. Shalom, *Angew. Chem., Int. Ed.*, 2015, **127**, 12538–12542.
12 Y. F. Xu, M. R. Gao, Y. R. Zheng, J. Jiang and S. H. Yu, *Angew. Chem., Int. Ed.*, 2013, **52**, 8546–8550.
13 Z. Zhang, R. Dua, L. Zhang, H. Zhu, H. Zhang and P. Wang, *ACS Nano*, 2013, **7**, 1709–1717.
14 M. L. Helm, M. P. Stewart, R. M. Bullock, M. R. DuBois and D. L. DuBois, *Science*, 2011, **333**, 863–866.
15 R. M. Bullock, A. M. Appel and M. L. Helm, *Chem. Commun.*, 2014, **50**, 3125–3143.
16 G. M. Jacobsen, J. Y. Yang, B. Twamley, A. D. Wilson, R. M. Bullock, M. R. DuBois and D. L. DuBois, *Energy Environ. Sci.*, 2008, **1**, 167–174.
17 M.-H. Ho, M. O'Hagan, M. Dupuis, D. L. DuBois, R. M. Bullock, W. J. Shaw and S. Raugei, *Dalton Trans.*, 2015, **44**, 10969–10979.
18 N. M. Muresan, J. Willkomm, D. Mersch, Y. Vaynzof and E. Reisner, *Angew. Chem., Int. Ed.*, 2012, **124**, 12921–12925.
19 M. J. Rose, H. B. Gray and J. R. Winkler, *J. Am. Chem. Soc.*, 2012, **134**, 8310–8313.
20 D. P. Estes, D. C. Grills and J. R. Norton, *J. Am. Chem. Soc.*, 2014, **136**, 17362–17365.
21 S. Mandal, S. Shikano, Y. Yamada, Y.-M. Lee, W. Nam, A. Llobet and S. Fukuzumi, *J. Am. Chem. Soc.*, 2013, **135**, 15294–15297.
22 G. Connor, K. Mayer, C. Tribble and W. McNamara, *Inorg. Chem.*, 2014, **53**, 5408–5410.
23 P. Du and R. Eisenberg, *Energy Environ. Sci.*, 2012, **5**, 6012–6021.
24 T. R. Simmons, G. Berggren, M. Bacchi, M. Fontecave and V. Artero, *Coord. Chem. Rev.*, 2014, **270–271**, 127–150.
25 C. S. Letko, J. A. Panetier, M. Head-Gordon and T. D. Tilley, *J. Am. Chem. Soc.*, 2014, **136**, 9364–9376.
26 L. Gan, T. L. Groy, P. Tarakeshwar, S. K. Mazinani, J. Shearer, V. Mujica and A. K. Jones, *J. Am. Chem. Soc.*, 2015, **137**, 1109–1115.
27 D. J. Graham and D. G. Nocera, *Organometallics*, 2014, **33**, 4994–5001.
28 H. I. Karunadasa, C. J. Chang and J. R. Long, *Nature*, 2010, **464**, 1329–1333.
29 W. M. Singh, T. Baine, S. Kudo, S. Tian, X. A. N. Ma, H. Zhou, N. J. DeYonker, T. C. Pham, J. C. Bollinger and D. L. Baker, *Angew. Chem., Int. Ed.*, 2012, **124**, 6043–6046.
30 L. Chen, M. Wang, K. Han, P. Zhang, F. Gloaguen and L. Sun, *Energy Environ. Sci.*, 2014, **7**, 329–334.
31 H. Chen, Z. Sun, S. Ye, D. Lu and P. Du, *J. Mater. Chem. A*, 2015, **3**, 15729–15737.
32 C. Floriani and G. Fachinetti, *J. Chem. Soc., Chem. Commun.*, 1974, 615–616.
33 O. F. Schall, K. Robinson, J. L. Atwood and G. W. Gokel, *J. Am. Chem. Soc.*, 1993, **115**, 5962–5969.
34 S. T. Meally, C. McDonald, P. Kealy, S. M. Taylor, E. K. Brechin and L. F. Jones, *Dalton Trans.*, 2012, **41**, 5610–5616.
35 B. Choudary, T. Ramani, H. Maheswaran, L. Prashant, K. Ranganath and K. V. Kumar, *Adv. Synth. Catal.*, 2006, **348**, 493–498.
36 A. Schepartz and J. P. McDevitt, *J. Am. Chem. Soc.*, 1989, **111**, 5976–5977.
37 C. Costentin, M. Robert and J.-M. Saveant, *Chem. Soc. Rev.*, 2013, **42**, 2423–2436.
38 C. Costentin, H. Dridi and J.-M. Savéant, *J. Am. Chem. Soc.*, 2014, **136**, 13727–13734.
39 C. Costentin, S. Drouet, M. Robert and J.-M. Savéant, *J. Am. Chem. Soc.*, 2012, **134**, 11235–11242.
40 J. B. Geri and N. K. Szymczak, *J. Am. Chem. Soc.*, 2015, **137**, 12808–12814.
41 D. W. Shaffer, S. I. Johnson, A. L. Rheingold, J. W. Ziller, W. A. Goddard, R. J. Nielsen and J. Y. Yang, *Inorg. Chem.*, 2014, **53**, 13031–13041.
42 E. S. Rountree, B. D. McCarthy, T. T. Eisenhart and J. L. Dempsey, *Inorg. Chem.*, 2014, **53**, 9983–10002.
43 B. H. Solis, A. Maher, T. Honda, D. C. Powers, D. G. Nocera and S. Hammes-Schiffer, *ACS Catal.*, 2014, **4**, 4516–4526.
44 J. S. Kanady, E. Y. Tsui, M. W. Day and T. Agapie, *Science*, 2011, **333**, 733–736.
45 S. Bang, Y.-M. Lee, S. Hong, K.-B. Cho, Y. Nishida, M. S. Seo, R. Sarangi, S. Fukuzumi and W. Nam, *Nat. Chem.*, 2014, **6**, 934–940.
46 T. D. Harris, H. S. Soo, C. J. Chang and J. R. Long, *Inorg. Chim. Acta*, 2011, **369**, 91–96.
47 C. A. Caputo, M. A. Gross, V. W. Lau, C. Cavazza, B. V. Lotsch and E. Reisner, *Angew. Chem., Int. Ed.*, 2014, **126**, 11722–11726.
48 S. K. Muduli, S. Wang, S. Chen, C. F. Ng, C. H. A. Huan, T. C. Sum and H. S. Soo, *Beilstein J. Nanotechnol.*, 2014, **5**, 517–523.